Nuclear Engineering and Technology 58 (2026) 103943

Contents lists available at ScienceDirect

Nuclear Engineering and Technology

journal homepage: www.elsevier.com/locate/net

Original Article

# Design optimization of a liquid sodium magnetohydrodynamic circulation system for a 20 MWe micro-nuclear reactor

Tae Uk Kang [1], Hee Reyoung Kim [*]

*Ulsan National Institute of Science and Technology, 50, UNIST-gil, Ulsan, 44919, Republic of Korea*

ARTICLE INFO

*Keywords:*
Lead–bismuth eutectic
Liquid sodium
Optimization
Small modular reactor (SMR)
Micro-nuclear reactor (NMR)

ABSTRACT

This study was presented the design optimization and numerical analysis of a sodium magnetohydrodynamic (MHD) circulation system intended for an all-in-one, liquid-sodium-cooled micro-nuclear reactor. Generally, given the compact size and high heat flux associated with microreactors, a stable and efficient cooling system is essential. MHD-based liquid metal circulation has emerged as a promising solution to this challenge. To determine the optimal MHD system configuration, an equivalent circuit-based fluid flow model was employed in this study. The system was designed to deliver a mass flow rate of 360 kg/s and a pressure head of 73 kPa at an operating temperature of 250 °C. The input power required for circulation was calculated to be 597 kW, which corresponds to approximately 3 % of the reactor's total electrical output of 20 MWe. These results demonstrate that the optimized design variables can enable the realization of a practical and energy-efficient MHD-based sodium cooling system with minimized input power and reduced energy losses, thereby supporting the broader implementation of micro-nuclear reactor technologies.

## 1. Introduction

In recent years, small modular reactors (SMRs) have garnered increasing global attention as a promising means of addressing the rising demand for clean, sustainable, and flexible energy production. Among the various types of advanced SMR technologies, sodium-cooled designs have attracted particular attention owing to their improved safety, high thermal efficiency, and nuclear waste recycling potential.

However, despite these advantages, one of the persistent challenges in sodium-cooled reactor design lies in ensuring efficient and reliable coolant circulation while minimizing system complexity and power consumption. Conventional mechanical pumps require frequent maintenance and present potential failure points under high-temperature environment. Thus, an optimized magnetohydrodynamic (MHD) circulation system, capable of achieving high efficiency with reduced structural and operational burdens, is urgently required. In this study, such problem is specifically addressed by proposing and analyzing design optimization strategy for sodium-cooled microreactors.

A prominent developer of sodium-cooled SMRs is TerraPower, a United-States-based firm known for its innovation in next-generation nuclear technologies. TerraPower is currently developing a sodium-cooled SMR designed to generate 345 MW of carbon-free power while addressing challenges related to energy reliability and sustainability [1]. The reactor design incorporates an advanced magnetohydrodynamic (MHD) circulation system that enables efficient and reliable transport of liquid sodium coolant. By eliminating the need for mechanical pumps, this system reduces maintenance requirements and enhances reactor safety.

Expanding upon the recent advancements in SMR technology, this study focuses on a more compact nuclear solution: the integrated micro-nuclear reactor (NMR). Specifically, it examines an MHD circulation system that makes direct use of the NMR's external wall. Integrating this system into the reactor's external structure enhances efficiency, reduces system complexity, lowers costs, and decreases overall reactor size. Moreover, employing the external wall as the primary component for both circulation and thermal management further simplifies the reactor design and reduces material usage and manufacturing costs. **The optimization of this MHD system is presented as a practical response to the design issues noted above, providing a structured way to evaluate and enhance its performance.**

As global decarbonization efforts intensify, sodium-cooled SMRs remain at the forefront of a nuclear renaissance, offering transformative potential for countries seeking to transition their energy systems while

* Corresponding author.
*E-mail addresses:* rkdxodnr25@add.re.kr (T.U. Kang), kimhr@unist.ac.kr (H.R. Kim).
[1] Please note that the first author, Tae Uk Kang, is currently affiliated with the Agency for Defense Development (ADD), Daejeon, Republic of Korea

https://doi.org/10.1016/j.net.2025.103943
Received 27 April 2025; Received in revised form 8 September 2025; Accepted 27 September 2025
Available online 6 October 2025

**Nomenclature**

| | |
|---|---|
| B | Magnetic flux density [T] |
| D | Hydraulic diameter [m] |
| E | Electric field [V/m] |
| F | Force [kg · m/s$^2$] |
| f | Frequency [Hz] |
| g | Gravitational acceleration [m/s$^2$] |
| H | Magnetic field strength [A/m] |
| I | Electric current [A] |
| J | Current density [A/m$^2$] |
| L | Pipe length [m] |
| L' | Pump height [m] |
| P | Developed pressure [kPa] |
| $\Delta P_L$ | Pressure loss [kPa] |
| p | Number of pole pairs |
| Q | Flow rate [LPM] |
| $R$ | Electrical resistance [Ω] |
| $s$ | Slip [%] |
| $t$ | Time [s] |
| V | Volume [m$^3$] |
| $v$ | Fluid velocity [m/s] |
| $V_s$ | Synchronous velocity [m/s] |
| $X$ | Reactance [Ω] |
| $\mu$ | Magnetic permeability [H/m] |
| $\rho$ | Density [kg/m$^3$] |
| $\sigma$ | Electrical conductivity [1/(Ω·m)] |
| $\eta$ | Dynamic viscosity [m$^2$/s] |
| $\eta'$ | Darcy friction factor |
| $\delta$ | Skin depth [m] |
| $\tau$ | Pole pitch [mm] |

ensuring economic scalability and environmental safety. In this context, the present study investigates the technical features, operational benefits, and future prospects of sodium-cooled NMRs, emphasizing their role in supporting the transformation of global energy infrastructures.

One such system is the micro ubiquitous, rugged, accident-forgiving, non-proliferating, and ultra-lasting sustainer (MicroURANUS), an NMR classified as an SMR. This reactor features a thermal output of 60 MWt and a pool-type fast reactor core arranged in a hexagonal lattice [2]. To achieve a pressure of 73 kPa, the reactor requires a relatively low mass flow rate of 360 kg/s. Given that sodium remains in a liquid state above 700 °C, a reactor operating between 500 and 550 °C maintains an adequate thermal margin during accidents. Moreover, because sodium absorbs heat effectively, it provides stable thermal performance even during heat sink failure or coolant loss, helping to maintain safe core temperatures. In the event of a power failure, decay heat from the reactor core can still be dissipated through natural convection between the sodium and surrounding atmosphere. Building on these advantages, this study performs an optimization analysis of the electromagnetic and geometric variables of the MHD circulation system of the liquid-sodium-cooled, all-in-one MicroURANUS reactor [3].

## 2. Theoretical approach

An MHD pump operates based on the principle of the Lorentz force, which arises from the vector product of the induced current and magnetic field. An externally applied current creates a magnetic field, which in turn induces an electrical current in the liquid metal. This current is oriented perpendicular to the magnetic field.

Fig. 1(a) illustrates the MHD pump considered in this study. The pump is divided into two primary regions. The first region is the electromagnet section, comprising inner and outer cores along with copper coil windings. This section generates a time-varying sinusoidal magnetic field and is built from silicon steel sheets with high magnetic permeability and copper with low electrical resistance. When a three-phase current flows through the coil windings, it produces a sinusoidal magnetic field propagating axially. This field travels along the inner core and is induced in the toothed region of the E-shaped outer core, resulting in a radial magnetic field. Moreover, to minimize energy losses from ohmic dissipation, the pump incorporates stacked thin silicon steel sheets and oxygen-free copper with low electrical resistance. According to Faraday's law, a time-varying axial magnetic field induces a circumferential current in the conductive fluid flowing through the system. The interaction between this current and the radial magnetic field generates an outward electromagnetic (Lorentz) force in the flow direction. The second region houses the working fluid, which moves through a channel defined by inner and outer ducts. To accommodate the fluid's reactivity and preserve magnetic field integrity, SUS 316 stainless steel pipes are used. These pipes also ensure sufficient mechanical strength [4,5]. The corresponding circuit diagram is presented in Fig. 1(b).

Fig. 2 illustrates the schematic layout of the MicroURANUS system, where fluid motion is driven by the force generated from the MHD pump. The fluid rises from the bottom to the top of the reactor through natural convection and is continuously recirculated by the MHD system. The external MHD circulation unit, connected to the MicroURANUS containment vessel, comprises an outer core, inner core, coils, and flow channel ducts, as illustrated in Fig. 3. To optimize magnetic flux paths from the teeth of the pump's outer core, the inner core thickness and diameter are fixed at 80 mm and 2500 mm, respectively, in accordance with the geometric layout of the reactor core. Moreover, given that the pump is positioned beneath the steam generator, its height is constrained to 2500 mm. Within this constraint, the specific pump height is determined by the height of its magnetic poles. Notably, the pressure generated by the pump increases with increasing pole height and pitch length. However, increasing the pole length reduces the strength of the magnetic field. Taking these trade-offs into account—along with the thickness of the outer core teeth and coil width—the height of a single pump unit is set to 544.6 mm. Up to four such units can be connected in series [3]. Among the most critical parameters affecting MHD pump performance is the flow gap. As the gap narrows, magnetic flux density increases; however, beyond a certain point, density saturation occurs [6]. A gap that is too narrow may also degrade performance owing to the generation of forces opposing the fluid flow [7]. However, increasing the flow velocity reduces the pressure generated by the pump, thereby requiring higher input power. Conversely, if the flow gap becomes too wide, the magnetic flux density drops. Fig. 4 confirms that input power increases around a flow gap of 100 mm.

The magnetic field responsible for generating the Lorentz force is calculated using Maxwell's equations, which include Ampère's law, Faraday's law, and Gauss's law of magnetism, as presented in Eqs. (1)–(3) [8,9]. ANSYS Maxwell is used to perform calculations, considering a coolant channel of finite length.

$$\text{Ampere's law} : \nabla \times \vec{\boldsymbol{H}} = \vec{\boldsymbol{J}}, \tag{1}$$

$$\text{Faraday's law} : \nabla \times \vec{\mathbf{E}} = -\frac{\partial \vec{\boldsymbol{B}}}{\partial t}, \tag{2}$$

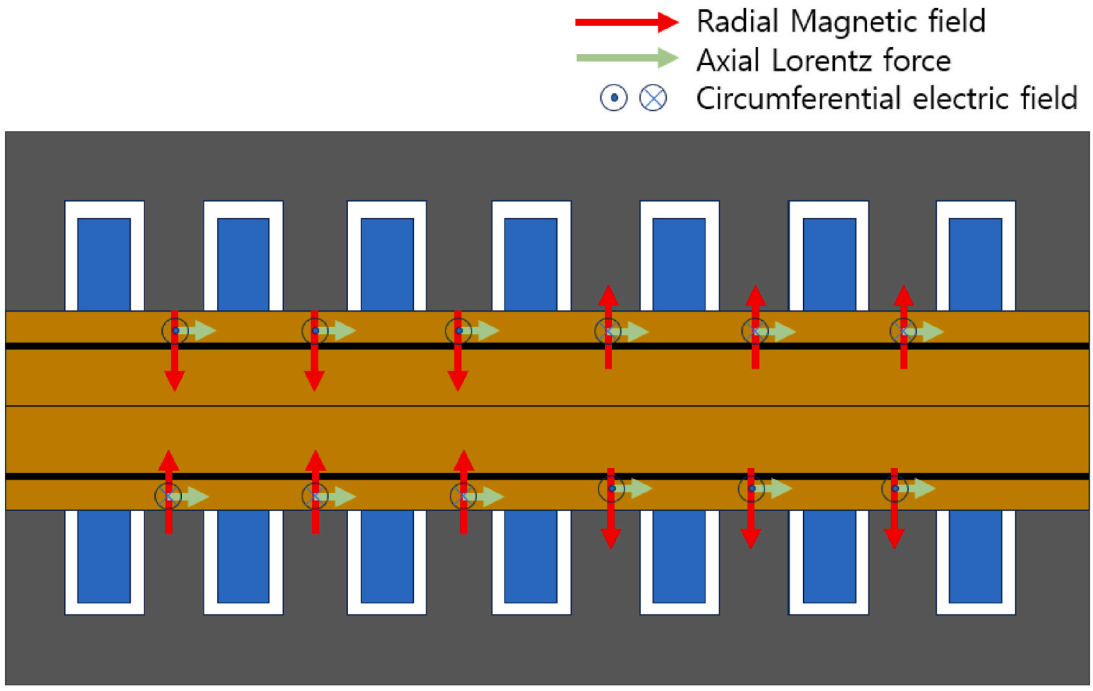


(a)

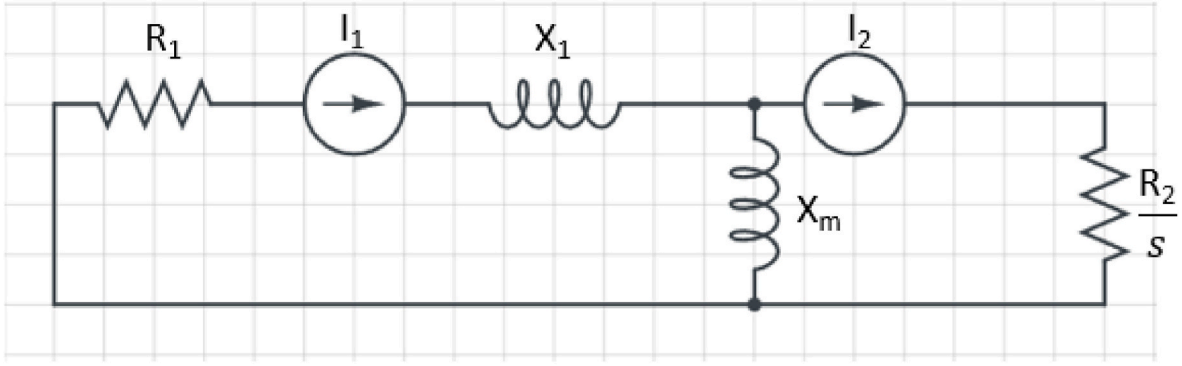


(b)

**Fig. 1.** Operating principle of the MHD pump.

$$\text{Gauss's law of magnetism} : \nabla \cdot \vec{\mathbf{B}} = 0. \tag{3}$$

Given sinusoidal time variation, the electric field, magnetic field, and current are expressed in as shown in Eq. (4), based on Eqs. (1)–(3).

$$\mathbf{E}(\mathrm{r},\theta,\mathrm{z}) = \mathrm{Re}\left[(E_r\hat{r} + E_\theta\hat{\theta} + E_z\hat{z})e^{iwt}\right],$$

$$\mathbf{B}(\mathrm{r},\theta,\mathrm{z}) = \mathrm{Re}\left[(B_r\hat{r} + B_\theta\hat{\theta} + B_z\hat{z})e^{iwt}\right], \tag{4}$$

$$\boldsymbol{J}(\mathrm{r},\theta,\mathrm{z}) = \mathrm{Re}\left[J_\theta e^{iwt}\right]\hat{\theta}.$$

Design variables for the MHD circulation system model are optimized using a combination of ANSYS Maxwell (electromagnetic), Fluent (thermal-hydraulic), and MATLAB code (one-dimensional optimization point). This analysis assumes a constant velocity at the wall boundary of the annular flow channel.

The Navier–Stokes equation is a nonlinear partial differential equation that yields the velocity and flow field of a fluid at a given time and

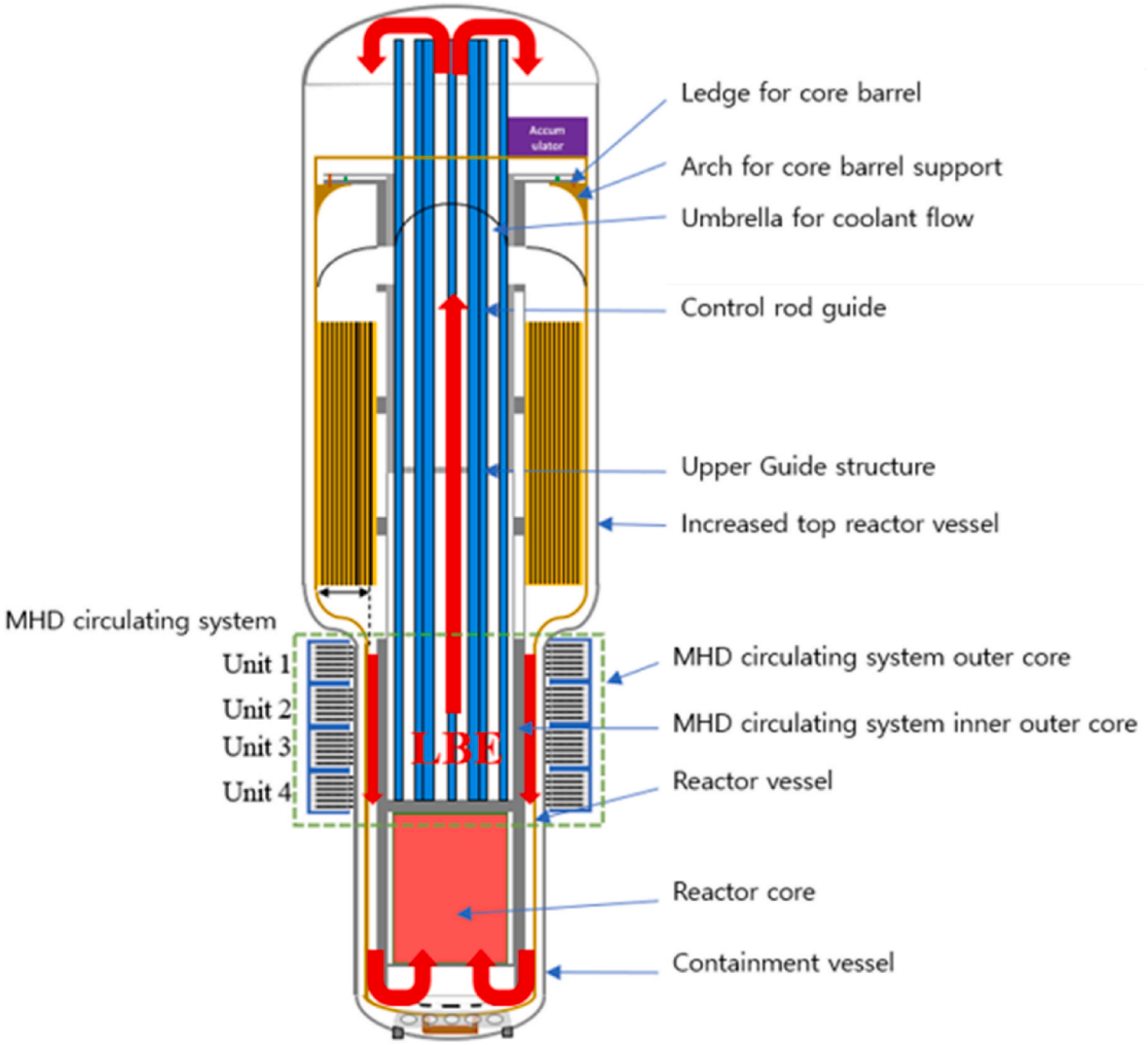


**Fig. 2.** Schematic of the MicroURANUS reactor with an integrated MHD circulation system.

spatial location. From this velocity field, other parameters such as flow rate can also be obtained. When the equation is expressed in cylindrical coordinates $r$, $\theta$, and $z$, it takes the component forms shown in Eqs. (5)–(7).

$$\rho\left(\frac{\partial v_r}{\partial t}+v_r\frac{\partial v_r}{\partial r}+\frac{v_\theta}{r}\frac{\partial v_r}{\partial \theta}+v_z\frac{\partial v_r}{\partial z}-\frac{v_\theta}{r}\right)=-\frac{\partial p}{\partial r}+\eta\left[\frac{1}{r}\frac{\partial}{\partial r}\left(r\frac{\partial v_r}{\partial r}\right)+\frac{1}{r^2}\frac{\partial^2 v_r}{\partial \theta^2}+\frac{\partial^2 v_r}{\partial z^2}-\frac{v_r}{r^2}-\frac{2}{r^2}\frac{\partial v_\theta}{\partial \theta}\right]+\frac{f_r}{V}, \tag{5}$$

$$\rho\left(\frac{\partial v_\theta}{\partial t}+v_r\frac{\partial v_\theta}{\partial r}+\frac{v_\theta}{r}\frac{\partial v_\theta}{\partial \theta}+v_z\frac{\partial v_\theta}{\partial z}-\frac{v_r v_\theta}{r}\right)=-\frac{1}{r}\frac{\partial p}{\partial \theta}+\eta\left[\frac{1}{r}\frac{\partial}{\partial r}\left(r\frac{\partial v_\theta}{\partial r}\right)+\frac{1}{r^2}\frac{\partial^2 v_\theta}{\partial \theta^2}+\frac{\partial^2 v_\theta}{\partial z^2}+\frac{v_\theta}{r^2}+\frac{2}{r^2}\frac{\partial v_r}{\partial \theta}\right]+\frac{f_\theta}{V}, \tag{6}$$

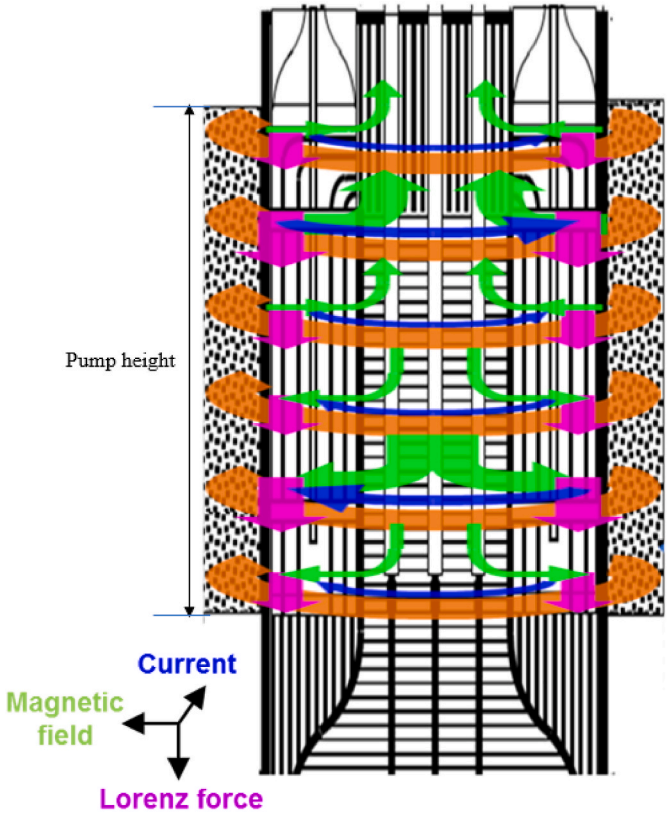


**Fig. 3.** Operation of the MHD circulation system within MicroURANUS (single-unit configuration).

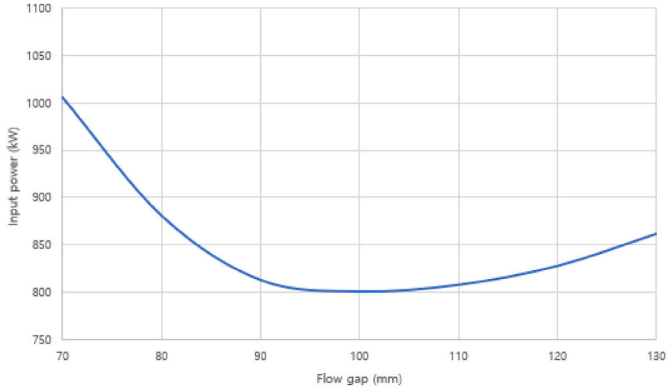


**Fig. 4.** Input power as a function of flow gap width.

$$\rho\left(\frac{\partial v_z}{\partial t}+v_r\frac{\partial v_z}{\partial r}+\frac{v_\theta}{r}\frac{\partial v_z}{\partial \theta}+v_z\frac{\partial v_z}{\partial z}\right)=-\frac{\partial p}{\partial z}+\eta\left[\frac{1}{r}\frac{\partial}{\partial r}\left(r\frac{\partial v_z}{\partial r}\right)+\frac{1}{r^2}\frac{\partial^2 v_z}{\partial \theta^2}+\frac{\partial^2 v_z}{\partial z^2}\right]+\frac{f_z}{V}. \tag{7}$$

The Lorentz or electromagnetic force is generated axially (z-direction) along the flow channel. It arises from the cross product of the azimuthal current and radial magnetic field produced by the MHD circulation system. This force, defined in Eq. (8), serves as the external source term in the Navier–Stokes equation.

$$\vec{\mathbf{F}}=\vec{\mathbf{J}}\times\vec{\boldsymbol{B}}=\left(\sigma E_\theta B_r-\sigma v_z {B_r}^2\right)\hat{\mathrm{z}}, \tag{8}$$

The pressure drop caused by friction along the pump flow path and the walls of the connected pipes during MHD circulation system operation is determined using the Darcy–Weisbach equation. In general, pressure losses arise from friction along the MHD circulation path; friction within the loop; minor losses associated with geometric flow path variations, such as internal valves and reducers; and gravitational effects. However, because the current analysis focuses exclusively on the pressure–flow characteristics of the MHD pump rather than the entire loop, non-frictional pressure loss components are excluded. Therefore, the pressure drop in the flow channel of the MHD circulation system is calculated using the Darcy–Weisbach equation, as shown in Eq. (9) [8].

$$\Delta P_L=\frac{\rho\eta' L v^2}{2D}. \tag{9}$$

The input power frequency influences the performance of the MHD circulation system through two primary effects: skin depth and slip. Variations in the electromagnetic field induce eddy currents near the conductor surface, and the associated skin depth is defined by Eq. (10):

$$\delta=\frac{1}{\sqrt{\pi f\sigma\mu}}. \tag{10}$$

Compared to DC MHD pumps, which usually have flow gaps measuring several millimeters, the MHD circulation system is equipped with a wider flow gap—typically ranging from several tens of millimeters to nearly 100 mm—making skin-effect-induced power loss a more important consideration. Notably, the skin effect reduces the effective cross-sectional area available for current flow, leading to increased power loss. To ensure efficient transmission of magnetic flux from the MHD circulation system across the flow gap, a frequency between 5 and 15 Hz is selected based on the skin depth of the pump material. Because this frequency is lower than typical commercial frequencies, power loss due to the skin effect can be minimized. Slip is defined as the relative difference between synchronous and flow velocities, as indicated in Eq. (11). Using the circuit diagram in Fig. 1(b), the pressure generated by the system can be expressed as a function of slip, as depicted in Eq. (12). The optimal slip value is determined through an optimization process. The diagram in Fig. 1(b) illustrates the relationship between slip and pressure generation, serving as the basis for determining optimal system performance.

$$s=\frac{V_s-V_f}{V_s}, \tag{11}$$

$$P=\frac{3I^2}{Q}\frac{R_2(1-s)}{s\left(\frac{{R_2}^2}{{X_m}^2 s^2}+1\right)}. \tag{12}$$

The pressure developed by the MHD circulation system is further optimized under a specified pole pitch range, as indicated in Eq. (13).

$$L'=2p\tau. \tag{13}$$

This study leverages established methodologies to ensure the reliability and robustness of its findings. Specifically, the adopted analytical approach aligns closely with the methods introduced by Kwak and Kim (2020) and Kang et al. (2022). Specifically, Kwak and Kim (2020) optimized the outer core to mitigate end effects in annular linear induction MHD pumps for Generation-IV sodium-cooled fast reactors. Their findings offered a solid basis for our MHD pump performance analysis [3,10]. Meanwhile, Kang et al. (2022) successfully optimized an extra-vessel MHD pump for lead–bismuth eutectic coolant circulation within small reactors, demonstrating the versatility and applicability of such techniques. Building upon these methodologies, the present study applies an equivalent circuit-based fluid flow analysis scheme to a different system: a sodium-cooled NMR with an external-wall-integrated MHD circulation system. By simplifying the complex interactions between electromagnetic forces and fluid motion, this equivalent circuit method enables efficient evaluation of key design parameters and system behavior. Given the proven accuracy of this analytical framework in

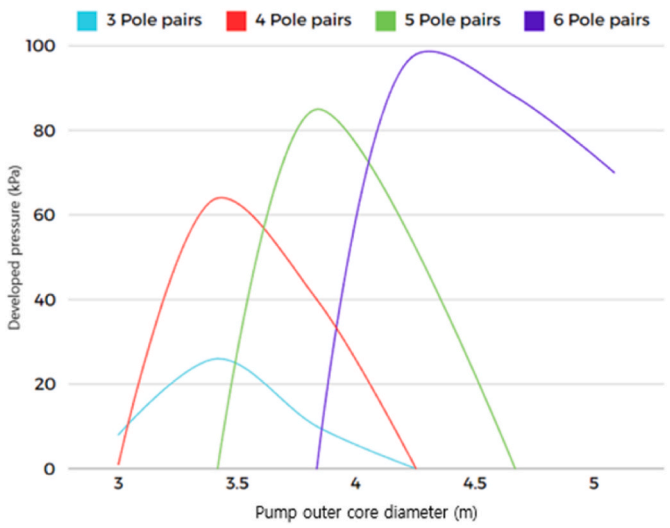


**Fig. 5.** Developed pressure as a function of outer core diameter and number of pole pairs at 5 Hz.

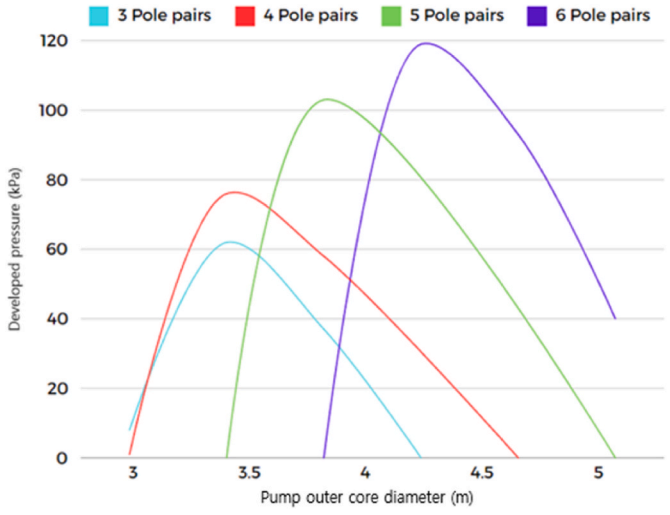


**Fig. 6.** Developed pressure as a function of outer core diameter and number of pole pairs at 10 Hz.

previous studies, its application herein reinforces the credibility of the results, ensuring the reliability and rigor of the resulting performance assessment. In this study, the performance of the MHD circulation system was examined under three frequency conditions—5 Hz, 10 Hz, and 15 Hz. Notably, considering these lower frequencies is critical, as they increase the skin depth and allow the magnetic field to penetrate more effectively into the flow channel. Moreover, MHD circulation systems typically operate at lower frequencies than those used in commercial power systems. This frequency range facilitates effective magnetic field application within the conducting medium, thereby enhancing circulation system performance [11,12].

To validate the results of this study and enhance its credibility, a comparative analysis was performed using data from previous studies on electromagnetic pumps. Specifically, the results from earlier studies were reproduced using the methodology proposed in this paper. In particular, employing the theoretical framework and computational models developed herein, key performance parameters—such as flow rate and pressure distribution—were recalculated and compared with those reported in the literature.

For validation, representative studies reporting both experimental

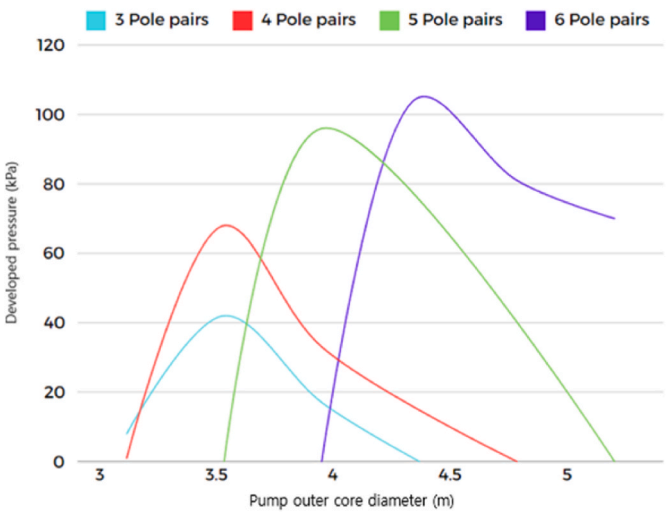


**Fig. 7.** Developed pressure as a function of outer core diameter and number of pole pairs at 15 Hz.

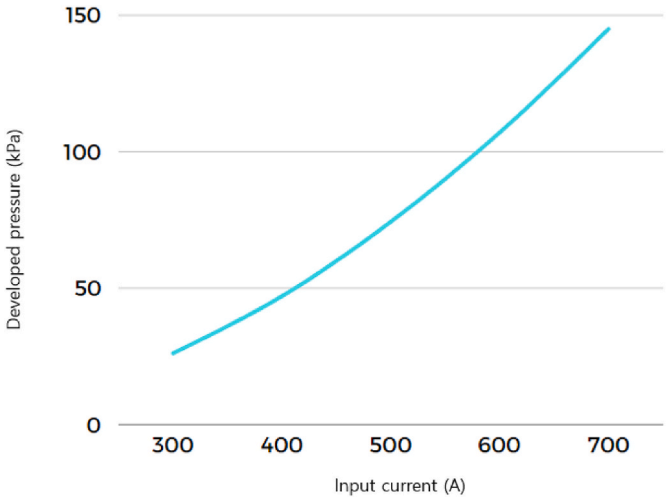


**Fig. 8.** Developed pressure as a function of input current.

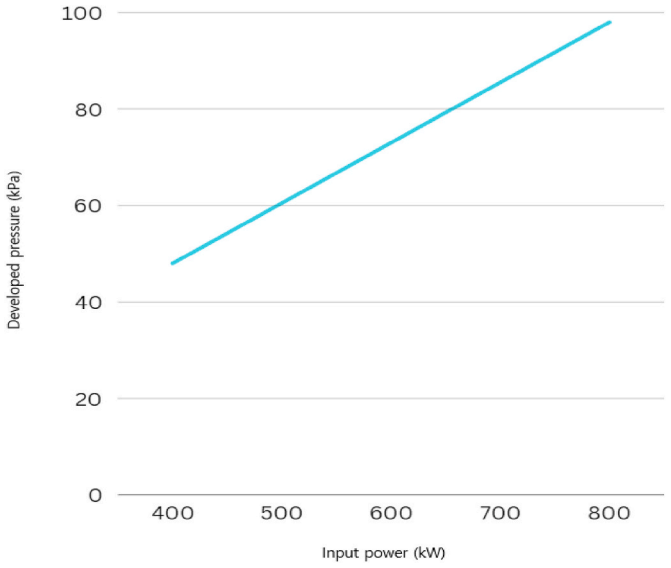


**Fig. 9.** Developed pressure as a function of input power.

**Table 1**
Specifications of the liquid sodium MHD circulation system.

| Design variable | | Unit | Value |
|---|---|---|---|
| Hydrodynamic | Mass flow rate | [kg/sec] | 360 |
| | Volumetric flow rate | [L/min] | 23,535 |
| | Developed pressure | [kPa] | 73 |
| | Temperature | [°C] | 250 |
| | Flow velocity | [m/sec] | 0.5 |
| | Reynolds number | [−] | 2,151,182 |
| Geometric | Pump height | [mm] | 2178 |
| | Outer core diameter of the pump | [mm] | 3432 |
| | Inner core diameter of the pump | [mm] | 2500 |
| | Flow gap width | [mm] | 100 |
| Electromagnetic | Input voltage | [V] | 1118 |
| | Number of pole pairs | [−] | 4 |
| | Input current | [A] | 500 |
| | Input frequency | [Hz] | 10 |
| | Number of coil turns | [−] | 20 |
| | Input power | [kW] | 597 |

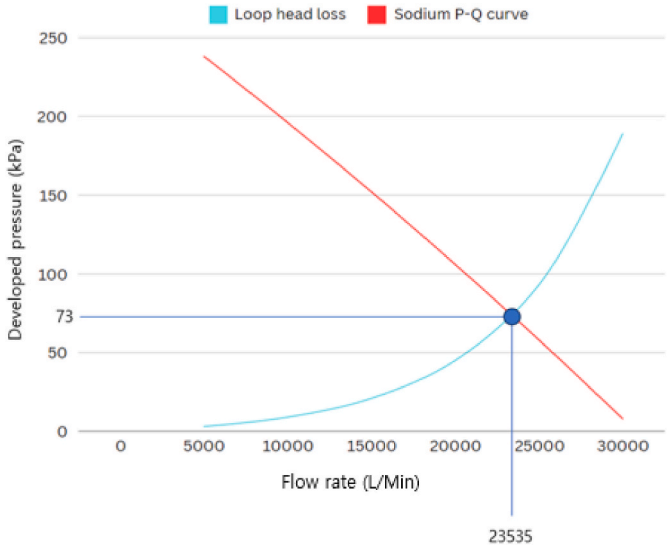


**Fig. 10.** Pressure–flow rate (P–Q) characteristics of the MHD circulation system.

and simulation results on electromagnetic pump performance were selected. A notable example is the study conducted by Kwak [4], which investigated similar systems and reported findings closely related to this study. Kwak's study was selected for its comparable operating conditions, especially the frequency (15 Hz) and temperature (322 °C), which closely match those used in the present study. Using identical boundary conditions and physical constraints, the method proposed in this study was applied to derive corresponding values.

## 3. Results and discussion

Figs. 5–7 depict the pressure generated by the MHD circulation system as a function of the outer core diameter of the pump for a scenario involving a fixed flow gap width of 100 mm and 20 coil windings. The presented results were obtained at frequencies of 5, 10, and 15 Hz for a core height of 2500 mm. As illustrated in the figures, increasing the number of pole pairs resulted in improved pump performance. Specifically, the developed pressure increased with the number of pole pairs. At 5 Hz, a maximum developed pressure of approximately 62 kPa was achieved with four pole pairs, and the optimal outer core diameter was approximately 3400 mm. At 10 Hz, the maximum pressure was 73 kPa with four pole pairs, with an optimal outer core diameter of 3432 mm. At 15 Hz, a maximum pressure of 68 kPa was achieved with four pole

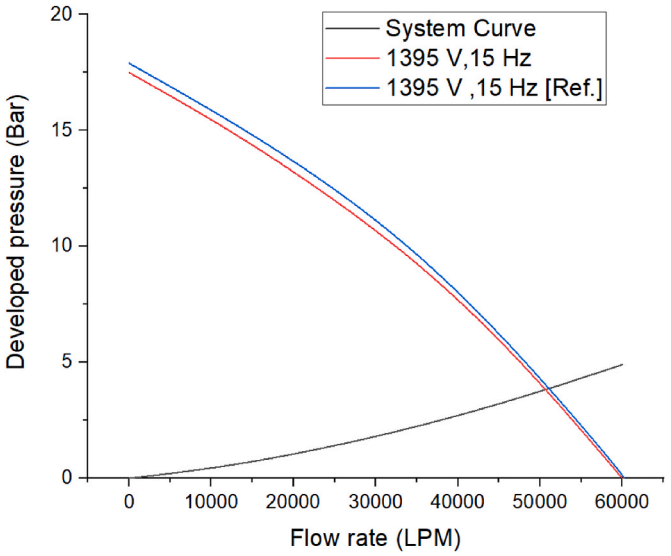


**Fig. 11.** Comparison of flow rate and developed pressure: reference study vs. proposed methodology.

**Table 2**
Comparison of MHD circulation system specifications: reference study vs. proposed methodology.

| Design variable | | Unit | Reference study | Proposed methodology |
|---|---|---|---|---|
| Hydrodynamic | Volumetric flow rate | [L/min] | 51,600 | 50,847 |
| | Developed pressure | [kPa] | 360 | 355 |
| | Temperature | [°C] | 322 | 322 |
| | Flow velocity | [m/sec] | 9.39 | 9.25 |
| | Reynolds number | [−] | 3,080,000 | 3,035,053 |
| | Pump height | [mm] | 3000 | 3000 |
| Geometric | Outer core diameter of the pump | [mm] | 1000 | 1000 |
| | Inner core diameter of the pump | [mm] | 0.415 | 0.415 |
| | Flow gap width Flow gap | [mm] | 60.9 | 60.9 |
| | Input voltage | [V] | 1118 | 1118 |
| Electromagnetic | Number of pole pairs | [−] | 8 | 8 |
| | Input current | [A] | 184 | 184 |
| | Input frequency | [Hz] | 15 | 15 |
| | Number of coil turns | [−] | 36 | 36 |
| | Input power | [kW] | 648 | 648 |

pairs, and the optimal outer core diameter was 3530 mm. Thus, across all frequencies, the optimal outer core diameter consistently fell within the range of 3400–3500 mm. Furthermore, the optimal frequency and outer core diameter were identified as 10 Hz and 3432 mm, respectively. The developed pressure was then calculated using the corresponding current and voltage values.

As illustrated in Fig. 8, the developed pressure increased proportionally to the square of the input current between 300 and 700 A. The target developed pressure corresponded to an input current of approximately 500 A. In summary, a lower input current is preferable, provided that the target pressure is still achieved. Fig. 9 presents the developed pressure as a function of input power, revealing a proportional increase with rising power.

Based on the above findings, the optimal specifications for the

sodium-cooled MicroURANUS included an outer core height of 2178 mm, 20 coil windings, four pole pairs, a current of 500 A, and a power of 597 kW, as listed in Table 1. Fig. 10 presents the pressure–flow rate (P–Q) characteristics of the optimally designed MHD circulation system. Notably, as the developed pressure decreased with increasing flow rate, no unstable regions were observed. Specifically, at a flow rate of 23,585 L/min, the developed pressure equaled the head loss—that is, 73 kPa.

To validate the reliability of the proposed methodology, a comparative analysis was performed with existing studies on electromagnetic pumps. The robustness of the approach was evaluated by directly comparing the calculated results with previously reported values. Here, numerical analysis was conducted using COMSOL Multiphysics, enabling detailed modeling of the system's electromagnetic and fluid flow behavior. Fig. 11 compares the developed pressure and flow rate reported in the reference study with those obtained using the proposed methodology. The intersection point in the graph corresponds to the operating condition of the MHD circulation system, where both approaches yield similar results. Notably, the COMSOL-based simulation yielded a flow rate of 50,847 L/min, while the reference study reported a value of 51,600 L/min. The absolute difference of 753 L/min between the two values corresponds to approximately 1.46 % of the reference value. This minimal deviation indicates strong agreement between the computed and reference values, reinforcing the reliability of the proposed approach in predicting electromagnetic pump behavior. In Table 2, the Reynolds number calculated using the proposed approach was 3,035,053, while the reference study reported a value of 3,080,000. These values are in close agreement, further validating the accuracy of the proposed methodology.

Similarly, the developed pressure reported by the reference study was 360 kPa, while the value obtained in this study was 355 kPa. The slight difference between the two values can be attributed to variations in numerical assumptions and boundary conditions used in the computational model. Despite this minor deviation, the proposed methodology demonstrates strong consistency with existing research findings, confirming its reliability in predicting electromagnetic pump performance.

## 4. Conclusion

In this study, we optimized the design of a sodium MHD circulating system intended for a liquid-sodium-cooled all-in-one NMR with an electrical output of 20 MWe—an emerging candidate for next-generation power systems in global energy technology. The MHD system was designed to deliver a mass flow rate of 360 kg/s and a developed pressure of 73 kPa at an operating temperature of 250 °C. To maximize thermal integration, the circulation system was configured to functionally utilize the reactor's external wall directly. The input power required by the MHD circulation system was 597 kW, representing approximately 3 % of the reactor's total electrical output. These results confirm that liquid sodium coolant can effectively achieve the target developed pressure of 73 kPa while maintaining the necessary mass flow rate of 360 kg/s.

Overall, the optimized design variables established in this study provide a practical foundation for the actual implementation of a sodium MHD circulating system with minimized input power and reduced energy losses in MicroURANUS.

## CRediT authorship contribution statement

**Tae Uk Kang:** Writing – review & editing, Writing – original draft, Visualization, Validation, Methodology, Investigation, Funding acquisition, Formal analysis, Data curation, Conceptualization. **Hee Reyoung Kim:** Writing – review & editing, Supervision, Project administration, Funding acquisition, Formal analysis, Conceptualization.

## Declaration of competing interest

The authors declare the following financial interests/personal relationships which may be considered as potential competing interests: Hee Reyoung Kim reports financial support was provided by the Korea Institute of Energy Technology Evaluation and Planning and the Ministry of Trade, Industry & Energy (MOTIE) of the Republic of Korea. If there are other authors, they declare that they have no known competing financial interests or personal relationships that could have appeared to influence the work reported in this paper.

## Acknowledgments

This research was supported by the Korea Institute of Energy Technology Evaluation and Planning (KETEP) and the Ministry of Trade, Industry and Energy (MOTIE) of the Republic of Korea under Grant No. 20214000000410.

## References

[1] TerraPower, The next Generation of Power is here–the Natrium® Reactor and Energy Storage System, TerraPower, n.d.
[2] S.M. Kim, J.H. Cho, I.S. Hwang, The development of LBE integral test loop, HELIOS and tests by using HELIOS, in: Transactions of the Korean Nuclear Society Spring Meeting, Taebaek, Korea, 2011. May 26–27.
[3] T.U. Kang, J.S. Kwak, H.R. Kim, Optimization of an extra vessel electromagnetic pump for lead–bismuth eutectic coolant circulation in a non-refueling full-life small reactor, Nucl. Eng. Technol. 54 (2022) 3919–3927, https://doi.org/10.1016/j.net.2022.04.026.
[4] J. Kwak, H.R. Kim, Design optimization analysis of a large electromagnetic pump for sodium coolant transportation in PGSFR, Ann. Nucl. Energy 121 (2018) 62–67, https://doi.org/10.1016/j.anucene.2018.07.019.
[5] K. Aizawa, Y. Chikazawa, S. Kotake, K. Ara, R. Aizawa, H. Ota, Electromagnetic pumps for main cooling systems of commercialized sodium-cooled fast reactor, J. Nucl. Sci. Technol. 48 (2011) 344–352, https://doi.org/10.1080/18811248.2011.9711709.
[6] D. Soltanova, P. Baranov, V. Baranova, A. Chudinova, Simulating magnetic field of a ferromagnetic pipe underwater in COMSOL multiphysics, in: 2014 International Conference on Electromagnetics in Advanced Applications (ICEAA), IOP Conf. Ser. Mater. Sci. Eng. 93 (2015) 012023, https://doi.org/10.1088/1757-899X/93/1/012023.
[7] G.O. Brown, The history of the Darcy–Weisbach equation for pipe flow resistance, in: Environmental and Water Resources History, ASCE Civil Engineering Conference and Exposition, 2002, https://doi.org/10.1061/40650(2003)4. Washington, D.C., Nov. 3–6.
[8] H.R. Kim, J.S. Kwak, MHD design analysis of an annular linear induction electromagnetic pump for SFR thermal hydraulic experimental loop, Ann. Nucl. Energy 92 (2016) 127–135, https://doi.org/10.1016/j.anucene.2016.01.035.
[9] J. Kwak, H.R. Kim, Performance analysis of magnetohydrodynamic pump for sodium-cooled fast reactor thermal hydraulic experiment, Ann. Nucl. Energy 132 (2019) 191–198, https://doi.org/10.1016/j.anucene.2019.04.037.
[10] J. Kwak, H.R. Kim, Optimization of outer core to reduce end effect of annular linear induction electromagnetic pump in prototype Generation-IV sodium-cooled fast reactor, Nucl. Eng. Technol. 52 (2020) 1380–1385, https://doi.org/10.1016/j.net.2019.12.006.
[11] P. Sharma, L.S. Sivakumar, R.R. Prasad, D.K. Saxena, V.S. Kumar, B.K. Nashine, P. Kalyanasundaram, Design, development and testing of a large capacity annular linear induction pump, Energy Proc. 7 (2011) 622–629, https://doi.org/10.1016/j.egypro.2011.06.083.
[12] H. Araseki, I.R. Kirillov, G.V. Preslitsky, A.P. Ogorodnikov, Magnetohydrodynamic instability in annular linear induction pump: part I. Experiment and numerical analysis, Nucl. Eng. Des. 227 (2004) 29–50, https://doi.org/10.1016/j.nucengdes.2003.07.001.